Chapter 3. A Few Simple Problems

The objective of this chapter is to solve a few simple but very important particle dynamics problems that may be reduced to 1D motion. They notably include the famous "planetary" problem of two particles interacting via a spherically symmetric potential, and the classical particle scattering problem. In the process of solution, several methods that will be very essential for the analysis of more complex systems are also discussed.

3.1. One-dimensional and 1D-reducible systems

If a particle is confined to motion along a straight line (say, axis x), its position is completely determined by this coordinate. In this case, as we already know, the particle's Lagrangian function is given by Eq. (2.21):

$$L = T(\dot{x}) - U(x,t), \quad T(\dot{x}) = \frac{m}{2}\dot{x}^2, \tag{3.1}$$

so the Lagrange equation of motion given by Eq. (2.22),

$$m\ddot{x} = -\frac{\partial U(x,t)}{\partial x} \tag{3.2}$$

is just the x-component of the 2nd Newton's law.

It is convenient to discuss the dynamics of such *really-1D systems* as a part of a more general class of *effectively-1D systems*. This is a system whose position, due to either holonomic constraints and/or conservation laws, is also fully determined by one generalized coordinate q, and whose Lagrangian may be represented in a form similar to Eq. (1):

Effectively-1D system

$$\boxed{L = T_{\text{ef}}(\dot{q}) - U_{\text{ef}}(q,t), \qquad T_{\text{ef}} = \frac{m_{\text{ef}}}{2}\dot{q}^2,} \tag{3.3}$$

where m_{ef} is some constant which may be considered as the *effective mass* of the system, and the function U_{ef}, its *effective potential energy*. In this case, the Lagrange equation (2.19), describing the system's dynamics, has a form similar to Eq. (2):

$$m_{\text{ef}}\ddot{q} = -\frac{\partial U_{\text{ef}}(q,t)}{\partial q}. \tag{3.4}$$

As an example, let us return to our testbed system shown in Fig. 2.1. We have already seen that for this system, having one degree of freedom, the genuine kinetic energy T, expressed by the first of Eqs. (2.23), is *not* a quadratically-homogeneous function of the generalized velocity. However, the system's Lagrangian function (2.23) still may be represented in the form (3),

$$L = \frac{m}{2}R^2\dot{\theta}^2 + \frac{m}{2}R^2\omega^2\sin^2\theta + mgR\cos\theta + \text{const} \equiv T_{\text{ef}} - U_{\text{ef}}, \tag{3.5}$$

provided that we take

$$T_{\text{ef}} \equiv \frac{m}{2}R^2\dot{\theta}^2, \qquad U_{\text{ef}} \equiv -\frac{m}{2}R^2\omega^2\sin^2\theta - mgR\cos\theta + \text{const.} \tag{3.6}$$

In this new partitioning of the function L, which is legitimate because U_{ef} depends only on the generalized coordinate θ, but not on the corresponding generalized velocity, T_{ef} includes only a part of the genuine kinetic energy T of the bead, while U_{ef} includes not only its real potential energy U in the gravity field but also an additional term related to ring rotation. (As we will see in Sec. 4.6, this term may be interpreted as the effective potential energy due to the inertial centrifugal "force" arising at the problem's solution in the non-inertial reference frame rotating with the ring.)

Returning to the general case of effectively-1D systems with Lagrangians of the type (3), let us calculate their Hamiltonian function, using its definition (2.32):

$$H = \frac{\partial L}{\partial \dot{q}}\dot{q} - L = m_{\text{ef}}\dot{q}^2 - (T_{\text{ef}} - U_{\text{ef}}) = T_{\text{ef}} + U_{\text{ef}}. \tag{3.7}$$

So, H is expressed via T_{ef} and U_{ef} exactly as the energy E is expressed via genuine T and U.

3.2. Equilibrium and stability

Autonomous systems are defined as dynamic systems whose equations of motion do not depend on time explicitly. For the effectively-1D (and in particular the really-1D) systems obeying Eq. (4), this means that their function U_{ef}, and hence the Lagrangian function (3) should not depend on time explicitly. According to Eqs. (2.35), in such systems, the Hamiltonian function (7), i.e. the sum $T_{\text{ef}} + U_{\text{ef}}$, is an integral of motion. However, be careful! Generally, this conclusion is not valid for the genuine mechanical energy E of such a system; for example, as we already know from Sec. 2.2, for our testbed problem, with the generalized coordinate $q = \theta$ (Fig. 2.1), E is not conserved.

According to Eq. (4), an autonomous system, at appropriate initial conditions, may stay in equilibrium at one or several *stationary* (alternatively called *fixed*) *points* q_n, corresponding to either the minimum or a maximum of the effective potential energy (see Fig. 1):

$$\boxed{\frac{dU_{\text{ef}}}{dq}(q_n) = 0.} \tag{3.8}$$

Fixed-point condition

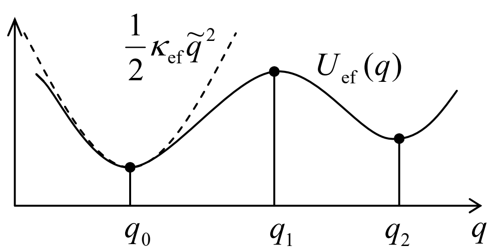

Fig. 3.1. An example of the effective potential energy profile near stable (q_0, q_2) and unstable (q_1) fixed points, and its quadratic approximation (10) near point q_0.

In order to explore the *stability* of such fixed points, let us analyze the dynamics of small deviations

$$\tilde{q}(t) \equiv q(t) - q_n \tag{3.9}$$

from one of such points. For that, let us expand the function U_{ef}(q) in the Taylor series at q_n:

$$U_{\text{ef}}(q) = U_{\text{ef}}(q_n) + \frac{dU_{\text{ef}}}{dq}(q_n)\tilde{q} + \frac{1}{2}\frac{d^2U_{\text{ef}}}{dq^2}(q_n)\tilde{q}^2 + \dots \tag{3.10}$$

The first term on the right-hand side, $U_{\text{ef}}(q_n)$, is an arbitrary constant and does not affect motion. The next term, linear in the deviation $\tilde{q}$, equals zero – see the fixed point's definition (8). Hence the fixed point's stability is determined by the next term, quadratic in $\tilde{q}$, more exactly by its coefficient,

$$\kappa_{\text{ef}} \equiv \frac{d^2U_{\text{ef}}}{dq^2}(q_n), \tag{3.11}$$

which is frequently called the *effective spring constant*. Indeed, neglecting the higher terms of the Taylor expansion (10),[1] we see that Eq. (4) takes the familiar form:

$$m_{\text{ef}}\ddot{\tilde{q}} + \kappa_{\text{ef}}\tilde{q} = 0. \tag{3.12}$$

I am confident that the reader of these notes knows everything about this equation, but since we will soon run into similar but more complex equations, let us review the formal procedure of its solution. From the mathematical standpoint, Eq. (12) is an ordinary linear differential equation of the second order, with constant coefficients. The general theory of such equations tells us that its general solution (for any initial conditions) may be represented as

$$\tilde{q}(t) = c_+ e^{\lambda_+ t} + c_- e^{\lambda_- t}, \tag{3.13}$$

where the constants $c_\pm$ are determined by initial conditions, while the so-called *characteristic exponents* $\lambda_\pm$ are completely defined by the equation itself. To calculate these exponents, it is sufficient to plug just one partial solution, $e^{\lambda t}$, into the equation. In our simple case (12), this yields the following *characteristic equation*:

$$m_{\text{ef}}\lambda^2 + \kappa_{\text{ef}} = 0. \tag{3.14}$$

If the ratio $k_{\text{ef}}/m_{\text{ef}}$ is positive, i.e. the fixed point corresponds to the minimum of potential energy (e.g., see points q_0 and q_2 in Fig. 1), the characteristic equation yields

$$\lambda_\pm = \pm i\omega_0, \qquad \text{with } \omega_0 \equiv \left(\frac{\kappa_{\text{ef}}}{m_{\text{ef}}}\right)^{1/2}, \tag{3.15}$$

(where i is the imaginary unit, $i^2 = -1$), so Eq. (13) describes *harmonic* (sinusoidal) oscillations of the system,[2]

$$\tilde{q}(t) = c_+ e^{+i\omega_0 t} + c_- e^{-i\omega_0 t} \equiv c_c \cos\omega_0 t + c_s \sin\omega_0 t, \tag{3.16}$$

---

[1] Those terms may be important only in very special cases when κ_{ef} is exactly zero, i.e. when a fixed point is also an *inflection point* of the function $U_{\text{ef}}(q)$.

[2] The reader should not be scared of the first form of (16), i.e. of the representation of a real variable (the deviation from equilibrium) via a sum of two complex functions. Indeed, any real initial conditions give $c_-^* = c_+$, so the sum is real for any t. An even simpler way to deal with such complex representations of real functions will be discussed in the beginning of Chapter 5, and then used throughout this series.

with the frequency ω_0, about the fixed point – which is thereby *stable*.[3] On the other hand, at the potential energy maximum ($k_{\text{ef}} < 0$, e.g., at point q_1 in Fig. 1), we get

$$\lambda_{\pm} = \pm\lambda, \quad \text{where } \lambda \equiv \left(\frac{|\kappa_{\text{ef}}|}{m_{\text{ef}}}\right)^{1/2}, \quad \text{so that } \tilde{q}(t) = c_+ e^{+\lambda t} + c_- e^{-\lambda t}. \qquad (3.17)$$

Since the solution has an exponentially growing part,[4] the fixed point is *unstable*.

Note that the *quadratic* expansion of function $U_{\text{ef}}(q)$, given by the truncation of Eq. (10) to the three displayed terms, is equivalent to a *linear* Taylor expansion of the effective force:

$$F_{\text{ef}} \equiv -\frac{dU_{\text{ef}}}{dq} \approx -\kappa_{\text{ef}}\tilde{q}, \qquad (3.18)$$

immediately resulting in the linear equation (12). Hence, to analyze the stability of a fixed point q_n, it is sufficient to *linearize* the equation of motion with respect to small deviations from the point, and study possible solutions of the resulting linear equation. This linearization procedure is typically simpler to carry out than the quadratic expansion (10).

As an example, let us return to our testbed problem (Fig. 2.1) whose function U_{ef} we already know – see the second of Eqs. (6). With it, the equation of motion (4) becomes

$$mR^2\ddot{\theta} = -\frac{dU_{\text{ef}}}{d\theta} = mR^2\left(\omega^2\cos\theta - \Omega^2\right)\sin\theta, \quad \text{i.e. } \ddot{\theta} = \left(\omega^2\cos\theta - \Omega^2\right)\sin\theta, \qquad (3.19)$$

where $\Omega \equiv (g/R)^{1/2}$ is the frequency of small oscillations of the system at $\omega = 0$ – see Eq. (2.26).[5] From Eq. (8), we see that on any 2π-long segment of the angle θ,[6] the system may have four fixed points; for example, on the half-open segment $(-\pi, +\pi]$ these points are

$$\theta_0 = 0, \qquad \theta_1 = \pi, \qquad \theta_{2,3} = \pm\cos^{-1}\frac{\Omega^2}{\omega^2}. \qquad (3.20)$$

The last two fixed points, corresponding to the bead shifted to either side of the rotating ring, exist only if the angular velocity ω of the rotation exceeds Ω. (In the limit of very fast rotation, $\omega >> \Omega$, Eq. (20) yields $\theta_{2,3} \to \pm\pi/2$, i.e. the stationary positions approach the horizontal diameter of the ring – in accordance with our physical intuition.)

To analyze the fixed point stability, we may again use Eq. (9), in the form $\theta = \theta_n + \tilde{\theta}$, plug it into Eq. (19), and Taylor-expand both trigonometric functions of θ up to the term linear in $\tilde{\theta}$:

$$\ddot{\tilde{\theta}} = \left[\omega^2\left(\cos\theta_n - \sin\theta_n\,\tilde{\theta}\right) - \Omega^2\right]\left(\sin\theta_n + \cos\theta_n\,\tilde{\theta}\right). \qquad (3.21)$$

---

[3] This particular type of stability, when the deviation from the equilibrium oscillates with a constant amplitude, neither growing nor decreasing in time, is called either *orbital*, or “neutral”, or “indifferent” *stability*.

[4] Mathematically, the growing part vanishes at some special (exact) initial conditions which give $c_+ = 0$. However, the futility of this argument for real physical systems should be obvious to anybody who has ever tried to balance a pencil on its sharp point.

[5] Note that Eq. (19) coincides with Eq. (2.25). This is a good sanity check illustrating that the procedure (5)-(6) of moving a term from the potential to the kinetic energy within the Lagrangian function is indeed legitimate.

[6] For this particular problem, the values of θ that differ by a multiple of 2π, are physically equivalent.

Generally, this equation may be linearized further by purging its right-hand side of the term proportional to $\tilde{\theta}^2$; however in this simple case, Eq. (21) is already convenient for analysis. In particular, for the fixed point $\theta_0 = 0$ (corresponding to the bead's position at the bottom of the ring), we have $\cos\theta_0 = 1$ and $\sin\theta_0 = 0$, so Eq. (21) is reduced to a linear differential equation

$$\ddot{\tilde{\theta}} = \left(\omega^2 - \Omega^2\right)\tilde{\theta}\ , \tag{3.22}$$

whose characteristic equation is similar to Eq. (14) and yields

$$\lambda^2 = \omega^2 - \Omega^2, \quad \text{for } \theta \approx \theta_0 . \tag{3.23a}$$

This result shows that if $\omega^2 < \Omega^2$, both roots λ are imaginary, so this fixed point is orbitally stable. However, if the rotation speed is increased so that $\Omega^2 < \omega^2$, the roots become real: $\lambda_\pm = \pm(\omega^2 - \Omega^2)^{1/2}$, with one of them positive, so the fixed point becomes unstable beyond this threshold, i.e. as soon as fixed points $\theta_{2,3}$ exist. Absolutely similar calculations for other fixed points yield

$$\lambda^2 = \begin{cases} \Omega^2 + \omega^2 > 0, & \text{for } \theta \approx \theta_1, \\ \Omega^2 - \omega^2, & \text{for } \theta \approx \theta_{2,3} . \end{cases} \tag{3.23b}$$

These results show that the fixed point θ_1 (the bead on the top of the ring) is always unstable – just as we could foresee, while the side fixed points $\theta_{2,3}$ are orbitally stable as soon as they exist – at $\Omega^2 < \omega^2$.

Thus, our fixed-point analysis may be summarized very simply: an increase of the ring rotation speed ω beyond a certain threshold value, equal to Ω given by Eq. (2.26), causes the bead to move to one of the ring sides, oscillating about one of the fixed points $\theta_{2,3}$. Together with the rotation about the vertical axis, this motion yields quite a complex (generally, open) spatial trajectory as observed from a lab frame, so it is fascinating that we could analyze it quantitatively in such a simple way.

Later in this course, we will repeatedly use the linearization of the equations of motion for the analysis of the stability of more complex dynamic systems, including those with energy dissipation.

3.3. Hamiltonian 1D systems

Autonomous systems that are described by time-independent Lagrangians are frequently called *Hamiltonian* ones because their Hamiltonian function H (again, not necessarily equal to the genuine mechanical energy E!) is conserved. In our current 1D case, described by Eq. (3),

$$H = \frac{m_{\text{ef}}}{2}\dot{q}^2 + U_{\text{ef}}(q) = \text{const} . \tag{3.24}$$

From a mathematical standpoint, this conservation law is just the first integral of motion. Solving Eq. (24) for $\dot{q}$, we get the first-order differential equation,

$$\frac{dq}{dt} = \pm\left\{\frac{2}{m_{\text{ef}}}\left[H - U_{\text{ef}}(q)\right]\right\}^{1/2}, \qquad \text{i.e. } \pm\left(\frac{m_{\text{ef}}}{2}\right)^{1/2}\frac{dq}{\left[H - U_{\text{ef}}(q)\right]^{1/2}} = dt , \tag{3.25}$$

which may be readily integrated:

$$\pm\left(\frac{m_{\text{ef}}}{2}\right)^{1/2}\int_{q(t_0)}^{q(t)}\frac{dq'}{\left[H-U_{\text{ef}}(q')\right]^{1/2}}=t-t_0\,. \tag{3.26}$$

Since the constant H (as well as the proper sign before the integral – see below) is fixed by initial conditions, Eq. (26) gives the reciprocal form, $t = t(q)$, of the desired law of system motion, $q(t)$. Of course, for any particular problem, the integral in Eq. (26) still has to be worked out, either analytically or numerically, but even the latter procedure is typically much easier than the numerical integration of the initial, second-order differential equation of motion, because at the addition of many values (to which any numerical integration is reduced[7]) the rounding errors are effectively averaged out.

Moreover, Eq. (25) also allows a general classification of 1D system motion. Indeed:

(i) If $H > U_{\text{ef}}(q)$ in the whole range of our interest, the effective kinetic energy T_{ef} (3) is always positive. Hence the derivative dq/dt cannot change its sign, so this effective velocity retains the sign it had initially. This is an unbound motion in one direction (Fig. 2a).

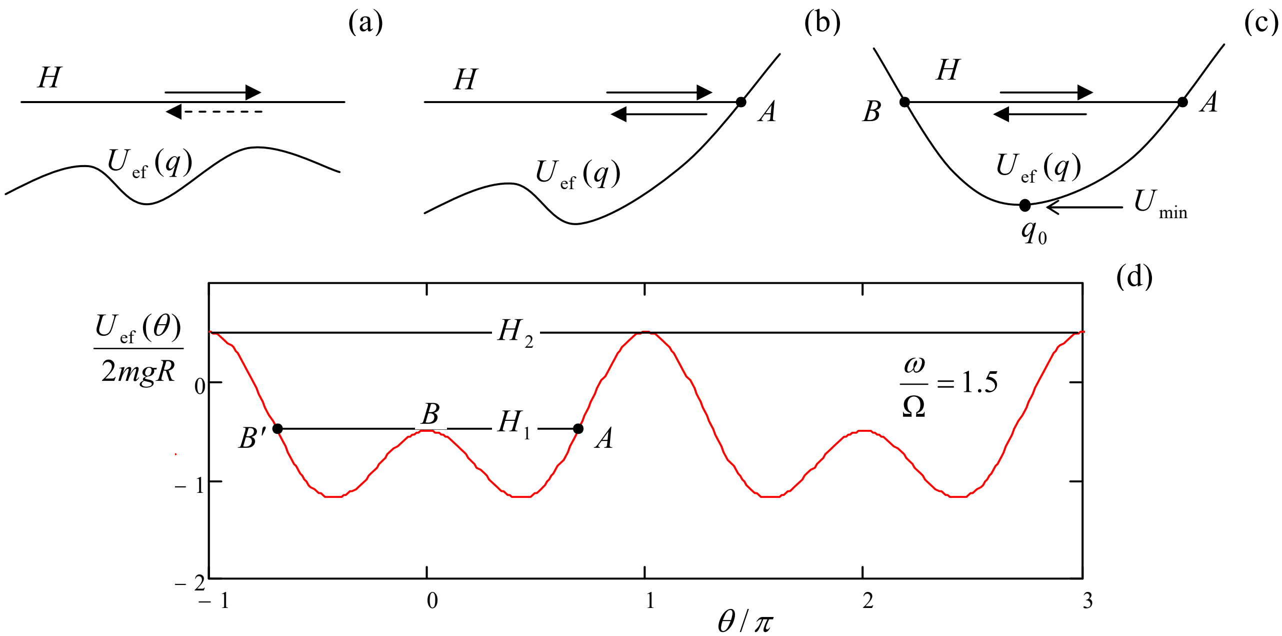

Fig. 3.2. Graphical representations of Eq. (25) for three different cases: (a) an unbound motion, with the velocity sign conserved, (b) a reflection from a "classical turning point", accompanied by the velocity sign change, and (c) bound, periodic motion between two turning points – schematically. (d) The effective potential energy (6) of the bead on the rotating ring (Fig. 2.1) for a particular case with $\Omega^2 < \omega^2$.

(ii) Now let the particle approach a *classical turning point A* where $H = U_{\text{ef}}(q)$ – see Fig. 2b.[8] According to Eq. (25), at that point, the particle velocity vanishes, while its acceleration, according to Eq. (4), is still finite. This means that the particle's velocity sign changes its sign at this point, i.e. it is *reflected* from it.

[7] See, e.g., MA Eqs. (5.2) and (5.3).

[8] This terminology comes from quantum mechanics, which shows that a particle (or rather its wavefunction) actually can, to a certain extent, penetrate "classically forbidden" regions where $H < U_{\text{ef}}(q)$.

(iii) If, after the reflection from some point A, the particle runs into another classical turning point B (Fig. 2c), the reflection process is repeated again and again, so the particle is bound to a periodic motion between two turning points.

The last case of *periodic oscillations* presents a large conceptual and practical interest, and the whole of Chapter 5 will be devoted to a detailed analysis of this phenomenon and numerous associated effects. Here I will only note that for an autonomous Hamiltonian system described by Eq. (4), Eq. (26) immediately enables the calculation of the oscillation period:

Oscillation period

$$\boxed{\mathcal{T} = 2\left(\frac{m_{\text{ef}}}{2}\right)^{1/2}\int_B^A \frac{dq}{[H - U_{\text{ef}}(q)]^{1/2}},} \tag{3.27}$$

where the additional front factor 2 accounts for two time intervals: of the motion from B to A and back – see Fig. 2c. Indeed, according to Eq. (25), at each classically allowed point q, the velocity's magnitude is the same, so these time intervals are equal to each other.

(Note that the dependence of points A and B on H is not necessarily continuous. For example, for our testbed problem, whose effective potential energy is plotted in Fig. 2d for a particular value of $\omega > \Omega$, a gradual increase of H leads to a sudden jump, at $H = H_1$, of the point B to a new position B', corresponding to a sudden switch from oscillations about one fixed point $\theta_{2,3}$ to oscillations about two adjacent fixed points – before the beginning of a persistent rotation around the ring at $H > H_2$.)

Now let us consider a particular, but a very important limit of Eq. (27). As Fig. 2c shows, if H is reduced to approach U_{min}, the periodic oscillations take place at the very bottom of this *potential well*, about a stable fixed point q_0. Hence, if the potential energy profile is smooth enough, we may limit the Taylor expansion (10) to the displayed quadratic term. Plugging it into Eq. (27), and using the mirror symmetry of this particular problem about the fixed point q_0, we get

$$\mathcal{T} = 4\left(\frac{m_{\text{ef}}}{2}\right)^{1/2}\int_0^A \frac{d\tilde{q}}{\left[H - \left(U_{\text{min}} + \kappa_{\text{ef}}\tilde{q}^2/2\right)\right]^{1/2}} = \frac{4}{\omega_0}I, \qquad \text{with } I \equiv \int_0^1 \frac{d\xi}{\left(1-\xi^2\right)^{1/2}}, \tag{3.28}$$

where $\xi \equiv \tilde{q}/A$, with $A \equiv (2/\kappa_{\text{ef}})^{1/2}(H - U_{\text{min}})^{1/2}$ being the classical turning point, i.e. the oscillation amplitude, and ω_0 the frequency given by Eq. (15). Taking into account that the elementary integral I in that equation equals $\pi/2$,[9] we finally get

$$\mathcal{T} = \frac{2\pi}{\omega_0}, \tag{3.29}$$

as it should be for the harmonic oscillations (16). Note that the oscillation period does not depend on the oscillation amplitude A, i.e. on the difference $(H - U_{\text{min}})$ – while it is sufficiently small.

3.4. Planetary problems

Leaving a more detailed study of oscillations for Chapter 5, let us now discuss the so-called *planetary systems*[10] whose description, somewhat surprisingly, may be also reduced to an effectively 1D

[9] Indeed, introducing a new variable ζ as $\xi \equiv \sin\zeta$, we get $d\xi = \cos\zeta\, d\zeta = (1-\xi^2)^{1/2}\, d\zeta$, so that the function under the integral is just $d\zeta$, and its limits are $\zeta = 0$ and $\zeta = \pi/2$.

problem. Indeed, consider two particles that interact via a conservative central force $\mathbf{F}_{21} = -\mathbf{F}_{12} = \mathbf{n}_r F(r)$, where r and $\mathbf{n}_r$ are, respectively, the magnitude and the direction of the *distance vector* $\mathbf{r} \equiv \mathbf{r}_1 - \mathbf{r}_2$ connecting the two particles (Fig. 3).

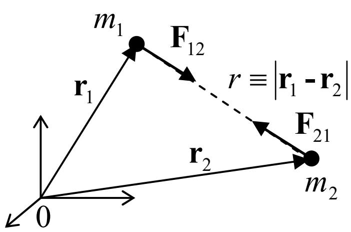

Fig. 3.3. Vectors in the planetary problem.

Generally, two particles moving without constraints in 3D space, have 3 + 3 = 6 degrees of freedom, which may be described, e.g., by their Cartesian coordinates $\{x_1, y_1, z_1, x_2, y_2, z_2\}$ However, for this particular form of interaction, the following series of tricks allows the number of essential degrees of freedom to be reduced to just one.

First, the conservative force of particle interaction may be described by a time-independent potential energy $U(r)$, such that $F(r) = -\partial U(r)/\partial r$.[11] Hence the Lagrangian function of the system is

$$L \equiv T - U(r) = \frac{m_1}{2}\dot{\mathbf{r}}_1^2 + \frac{m_2}{2}\dot{\mathbf{r}}_2^2 - U(r). \tag{3.30}$$

Let us perform the transfer from the initial six scalar coordinates of the particles to the following six generalized coordinates: three Cartesian components of the distance vector

$$\mathbf{r} \equiv \mathbf{r}_1 - \mathbf{r}_2, \tag{3.31}$$

and three scalar components of the following vector:

$$\boxed{\mathbf{R} \equiv \frac{m_1\mathbf{r}_1 + m_2\mathbf{r}_2}{M}, \quad \text{with } M \equiv m_1 + m_2,} \tag{3.32}$$

Center of mass

which defines the position of the *center of mass* of the system, with the total mass M. Solving the system of two linear equations (31) and (32) for $\mathbf{r}_1$ and $\mathbf{r}_2$, we get

$$\mathbf{r}_1 = \mathbf{R} + \frac{m_2}{M}\mathbf{r}, \qquad \mathbf{r}_2 = \mathbf{R} - \frac{m_1}{M}\mathbf{r}. \tag{3.33}$$

Plugging these relations into Eq. (30), we see that it is reduced to

$$L = \frac{M}{2}\dot{\mathbf{R}}^2 + \frac{m}{2}\dot{\mathbf{r}}^2 - U(r), \tag{3.34}$$

where m is the so-called *reduced mass*:

$$\boxed{m \equiv \frac{m_1 m_2}{M}, \quad \text{so that } \frac{1}{m} \equiv \frac{1}{m_1} + \frac{1}{m_2}.} \tag{3.35}$$

Reduced mass

---

[10] This name is very conditional, because this group of problems includes, for example, charged particle scattering (see Sec. 3.7 below).

[11] See, e.g., MA Eq. (10.8) with $\partial/\partial\theta = \partial/\partial\varphi = 0$.

Note that according to Eq. (35), the reduced mass is lower than that of the lightest component of the two-body system. If one of $m_{1,2}$ is *much* less than its counterpart (like it is in most star-planet or planet-satellite systems), then with a good precision $m \approx \min\,[m_1, m_2]$.

Since the Lagrangian function (34) depends only on $\dot{\mathbf{R}}$ rather than $\mathbf{R}$ itself, according to our discussion in Sec. 2.4, all Cartesian components of R are cyclic coordinates, and the corresponding generalized momenta are conserved:

$$P_j \equiv \frac{\partial L}{\partial \dot{R}_j} \equiv M\dot{R}_j = \text{const}, \quad j = 1, 2, 3. \tag{3.36}$$

Physically, this is just the conservation law for the full momentum $\mathbf{P} \equiv M\mathbf{R}$ of our system, due to the absence of external forces. Actually, in the axiomatics used in Sec. 1.3 this law is postulated – see Eq. (1.10) – but now we may attribute the momentum $\mathbf{P}$ to a certain geometric point, with the center-of-mass radius vector $\mathbf{R}$. In particular, since according to Eq. (36) the center moves with a constant velocity in the inertial reference frame used to write Eq. (30), we may consider a new inertial frame with the origin at point $\mathbf{R}$. In this new frame, $\mathbf{R} \equiv 0$, so the vector $\mathbf{r}$ (and hence the scalar r) remain the same as in the old frame (because the frame transfer vector adds equally to $\mathbf{r}_1$ and $\mathbf{r}_2$, and cancels in $\mathbf{r} = \mathbf{r}_1 - \mathbf{r}_2$), and the Lagrangian (34) is now reduced to

$$L = \frac{m}{2}\dot{\mathbf{r}}^2 - U(r). \tag{3.37}$$

Thus our initial problem has been reduced to just three degrees of freedom – three scalar components of the vector $\mathbf{r}$. In other words, Eq. (37) shows that the dynamics of the vector $\mathbf{r}$ of our initial, two-particle system is identical to that of the radius vector of a *single particle* with the effective mass m, moving in the central potential field $U(r)$.

Two more degrees of freedom may be excluded from the planetary problem by noticing that according to Eq. (1.35), the angular momentum $\mathbf{L} = \mathbf{r}\times\mathbf{p}$ of our effective single particle of mass m is also conserved, both in magnitude and direction. Since the direction of $\mathbf{L}$ is, by its definition, perpendicular to both $\mathbf{r}$ and $\mathbf{v} = \mathbf{p}/m$, this means that the particle's motion is confined to the plane whose orientation is determined by the initial directions of the vectors $\mathbf{r}$ and $\mathbf{v}$. Hence we can completely describe the particle's position by just two coordinates in that plane, for example by the distance r to the origin, and the polar angle φ. In these coordinates, Eq. (37) takes the form identical to Eq. (2.49):

$$L = \frac{m}{2}\left(\dot{r}^2 + r^2\dot{\varphi}^2\right) - U(r)\,. \tag{3.38}$$

Moreover, the latter coordinate, polar angle φ, may be also eliminated by using the conservation of angular momentum's magnitude, in the form of Eq. (2.50): [12]

$$L_z = mr^2\dot{\varphi} = \text{const}. \tag{3.39}$$

A direct corollary of this conservation is the so-called 2^{nd} *Kepler's law*:[13] the radius vector $\mathbf{r}$ sweeps equal areas A in equal time periods. Indeed, in the linear approximation in $dA << A$, the area

[12] Here index z stands for the coordinate perpendicular to the motion plane. Since other components of the angular momentum equal zero, this index is not really necessary, but I will still use it – just to make a clear distinction between the angular momentum L_z and the Lagrangian function L.

differential dA is equal to the area of a narrow right triangle with the base being the arc differential $rd\varphi$, and the height equal to r – see Fig. 4. As a result, according to Eq. (39), the time derivative of the area,

$$\frac{dA}{dt} = \frac{r(rd\varphi)/2}{dt} \equiv \frac{1}{2}r^2\dot{\varphi} = \frac{L_z}{2m}, \tag{3.40}$$

remains constant. Since the factor $L_z/2m$ is constant, integration of this equation over an arbitrary (not necessarily small!) time interval Δt proves the 2nd Kepler's law: $A \propto \Delta t$.

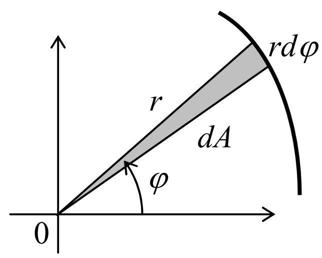

Fig. 3.4. The area differential dA in the polar coordinates.

Now note that since $\partial L/\partial t = 0$, the Hamiltonian function H is also conserved, and since, according to Eq. (38), the kinetic energy of the system is a quadratic-homogeneous function of the generalized velocities $\dot{r}$ and $\dot{\varphi}$, we have $H = E$, so the system's energy E,

$$E = \frac{m}{2}\dot{r}^2 + \frac{m}{2}r^2\dot{\varphi}^2 + U(r), \tag{3.41}$$

is also the first integral of motion.[14] However, according to Eq. (39), the second term on the right-hand side of Eq. (41) may be represented as

$$\frac{m}{2}r^2\dot{\varphi}^2 = \frac{L_z^2}{2mr^2}, \tag{3.42}$$

so the energy (41) may be expressed as that of a 1D particle moving along axis r,

$$E = \frac{m}{2}\dot{r}^2 + U_{\text{ef}}(r), \tag{3.43}$$

in the following effective potential:

$$\boxed{U_{\text{ef}}(r) \equiv U(r) + \frac{L_z^2}{2mr^2}.} \tag{3.44}$$

Effective potential energy

So the planetary motion problem has been reduced to the study of an effectively-1D system.[15]

[13] This is one of the three laws deduced, from the extremely detailed astronomical data collected by Tycho Brahe (1546-1601), by Johannes Kepler in the early 17th century. In turn, the three Kepler's laws have become the main basis for Newton's discovery, a few decades later, of the gravity law (1.15). That relentless march of physics…

[14] One may argue that this fact should have been evident earlier because the effective particle of mass m moves in a potential field $U(r)$, which conserves energy.

[15] Note that this reduction has been done in a way different from that used for our testbed problem (Fig. 2.1) in Sec. 2 above. (The reader is encouraged to analyze this difference.) To emphasize this fact, I will keep writing E instead of H here, though for the planetary problem we are discussing now, these two notions coincide.

Now we may proceed just like we did in Sec. 3, with due respect to the very specific effective potential (44) which, in particular, diverges at $r \to 0$ – besides the very special case of an exactly radial motion, $L_z = 0$. In particular, we may solve Eq. (43) for dr/dt to get

$$dt = \left(\frac{m}{2}\right)^{1/2} \frac{dr}{[E - U_{\text{ef}}(r)]^{1/2}}. \tag{3.45}$$

This equation enables us not only to get a direct relation between time t and distance r, similarly to Eq. (26),

$$t = \pm\left(\frac{m}{2}\right)^{1/2} \int \frac{dr}{[E - U_{\text{ef}}(r)]^{1/2}} = \pm\left(\frac{m}{2}\right)^{1/2} \int \frac{dr}{[E - U(r) - L_z^2/2mr^2]^{1/2}}, \tag{3.46}$$

but also do a similar calculation of the angle φ of the effective particle. Indeed, integrating Eq. (39),

$$\varphi \equiv \int \dot{\varphi}\, dt = \frac{L_z}{m} \int \frac{dt}{r^2}, \tag{3.47}$$

and plugging dt from Eq. (45), we get an explicit expression for the particle's trajectory $\varphi(r)$:

$$\varphi = \pm\frac{L_z}{(2m)^{1/2}} \int \frac{dr}{r^2[E - U_{\text{ef}}(r)]^{1/2}} = \pm\frac{L_z}{(2m)^{1/2}} \int \frac{dr}{r^2[E - U(r) - L_z^2/2mr^2]^{1/2}}. \tag{3.48}$$

Note that according to Eq. (39), the derivative $d\varphi/dt$ does *not* change sign at the reflection from any classical turning point $r \neq 0$, so, in contrast to Eq. (46), the sign on the right-hand side of Eq. (48) is uniquely determined by the initial conditions and cannot change during the motion.

Let us use these results, valid for any interaction law $U(r)$, for the planetary motion's classification. (Following a good tradition, in what follows I will select the arbitrary constant in the potential energy in the way to provide $U \to 0$ and hence $U_{\text{ef}} \to 0$, at $r \to \infty$.) The following cases should be distinguished.

If $U(r) < 0$, i.e. the particle interaction is *attractive* (as it always is in the case of gravity), and the divergence of the attractive potential at $r \to 0$ is faster than $1/r^2$, then $U_{\text{ef}}(r) \to -\infty$ at $r \to 0$, so at appropriate initial conditions the particle may drop on the center even if $L_z \neq 0$ – the event called the *capture*.[16] On the other hand, with $U(r)$ either converging or diverging slower than $1/r^2$, at $r \to 0$, the effective energy profile $U_{\text{ef}}(r)$ has the shape shown schematically in Fig. 5. This is true, in particular, for the very important case

Attractive Coulomb potential

$$\boxed{U(r) = -\frac{\alpha}{r}, \quad \text{with } \alpha > 0,} \tag{3.49}$$

which describes, in particular, the *Coulomb* (electrostatic) *interaction* of two particles with electric charges of opposite signs, and Newton's gravity law (1.15). This particular case will be analyzed in detail below, but for now, let us return to the analysis of an arbitrary attractive potential $U(r) < 0$ leading to the effective potential shown in Fig. 5 when the angular-momentum term in Eq. (44) dominates at small distances r.

---

[16] In order to analyze what exactly happens at the capture, i.e. at $r = 0$, we would need a model more specific than Eq. (30).

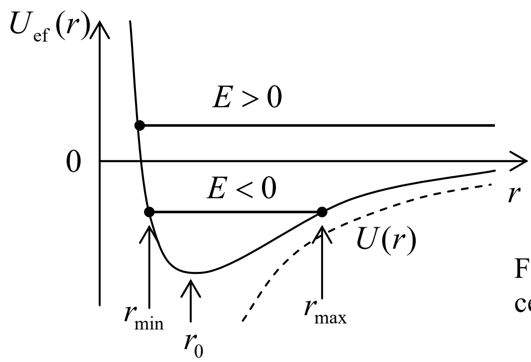

Fig. 3.5. Effective potential profile of an attractive central field, and two types of motion in it.

According to the analysis in Sec. 3, such potential profile, with a minimum at some distance r_0, may sustain two types of motion, depending on the energy E (determined by initial conditions):

(i) If $E > 0$, there is only one classical turning point where $E = U_{ef}$, so the distance r either grows with time from the very beginning or (if the initial value of $\dot{r}$ was negative) first decreases and then, after the reflection from the increasing potential U_{ef}, starts to grow indefinitely. The latter case, of course, describes the *scattering* of the effective particle by the attractive center.[17]

(ii) On the opposite, if the energy is within the range

$$U_{ef}(r_0) \leq E < 0, \tag{3.50}$$

the system moves periodically between two classical turning points r_{min} and r_{max} – see Fig. 5. These oscillations of the distance r correspond to the bound orbital motion of our effective particle about the attracting center.

Let us start with the discussion of the bound motion, with the energy within the range (50). If the energy has its minimal possible value,

$$E = U_{ef}(r_0) \equiv \min[U_{ef}(r)], \tag{3.51}$$

the distance cannot change, $r = r_0 = \text{const}$, so the particle's orbit is circular, with the radius r_0 satisfying the condition $dU_{ef}/dr = 0$. Using Eq. (44), we see that the condition for r_0 may be written as

$$\frac{L_z^2}{mr_0^3} = \left.\frac{dU}{dr}\right|_{r=r_0}. \tag{3.52}$$

Since at circular motion, the velocity $\mathbf{v}$ is perpendicular to the radius vector $\mathbf{r}$, L_z is just mr_0v, the left-hand side of Eq. (52) equals mv^2/r_0, while its right-hand side is just the magnitude of the attractive force, so this equality expresses the well-known 2[nd] Newton's law for the circular motion. Plugging this result into Eq. (47), we get a linear law of angle change, $\varphi = \omega t + \text{const}$, with the angular velocity

$$\omega = \frac{L_z}{mr_0^2} = \frac{v}{r_0}, \tag{3.53}$$

and hence the rotation period $\mathcal{T}_\varphi \equiv 2\pi/\omega$ obeys the elementary relation

[17] In the opposite case when the interaction is *repulsive*, $U(r) > 0$, the addition of the positive angular energy term only increases the trend, and the scattering scenario is the only one possible.

$$\mathcal{T}_\varphi = \frac{2\pi r_0}{v}. \qquad (3.54)$$

Now let the energy be above its minimum value (but still negative). Using Eq. (46) just as in Sec. 3, we see that the distance r oscillates with the period

$$\mathcal{T}_r = 2\left(\frac{m}{2}\right)^{1/2} \int_{r_{\min}}^{r_{\max}} \frac{dr}{[E - U(r) - L_z^2 / 2mr^2]^{1/2}}. \qquad (3.55)$$

This period is not necessarily equal to another period, $\mathcal{T}_\varphi$, that corresponds to the 2π-change of the angle. Indeed, according to Eq. (48), the change of the angle φ between two sequential points of the nearest approach,

$$|\Delta\varphi| = 2\frac{L_z}{(2m)^{1/2}} \int_{r_{\min}}^{r_{\max}} \frac{dr}{r^2\left[E - U(r) - L_z^2 / 2mr^2\right]^{1/2}}, \qquad (3.56)$$

is generally different from 2π. Hence, the general trajectory of the bound motion has a spiral shape – see, e.g., an illustration in Fig. 6.

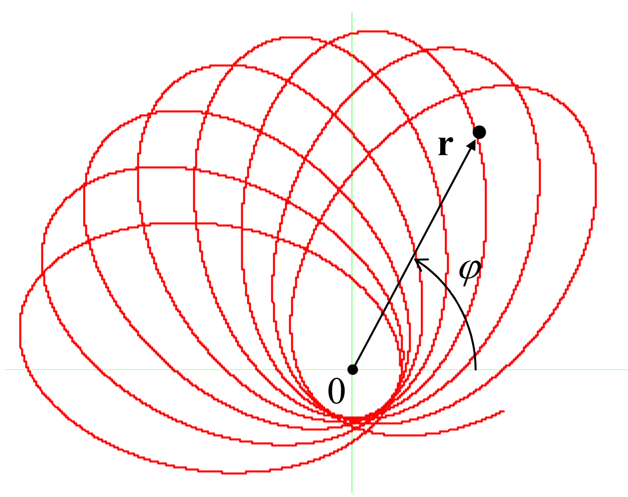

Fig. 3.6. A typical open orbit of a particle moving in a non-Coulomb central field.

The situation is special, however, for a very important particular case, namely that of the Coulomb potential described by Eq. (49).[18] Indeed, plugging this potential into Eq. (48), we get

$$\varphi = \pm \frac{L_z}{(2m)^{1/2}} \int \frac{dr}{r^2\left(E + \alpha / r - L_z^2 / 2mr^2\right)^{1/2}}. \qquad (3.57)$$

This is a table integral,[19] giving

$$\varphi = \pm \cos^{-1} \frac{L_z^2 / m\alpha r - 1}{\left(1 + 2EL_z^2 / m\alpha^2\right)^{1/2}} + \text{const.} \qquad (3.58)$$

[18] For the power-law interaction, $U \propto r^\nu$, the orbits are closed curves only if either $\nu = -1$ (the Coulomb potential) or $\nu = +2$ (the 3D harmonic oscillator) – the so-called *Bertrand theorem*, proved by J. Bertrand only in 1873.
[19] See, e.g., MA Eq. (6.3a).

Hence the reciprocal function, $r(\varphi)$, is 2π-periodic:

$$\boxed{r = \frac{p}{1 + e\cos(\varphi + \text{const})},} \tag{3.59}$$

Elliptic orbit and its parameters

so at $E < 0$, the orbit is a closed line characterized by the following parameters:[20]

$$\boxed{p \equiv \frac{L_z^2}{m\alpha}, \qquad e \equiv \left(1 + \frac{2EL_z^2}{m\alpha^2}\right)^{1/2}.} \tag{3.60}$$

The physical meaning of these parameters is very simple. Indeed, the general Eq. (52), in the Coulomb potential for which $dU/dr = \alpha/r^2$, shows that p is just the circular orbit radius[21] for the given L_z: $r_0 = L_z^2/m\alpha \equiv p$, so

$$\min[U_{\text{ef}}(r)] \equiv U_{\text{ef}}(r_0) = -\frac{\alpha^2 m}{2L_z^2}. \tag{3.61}$$

Using this equality together with the second of Eqs. (60), we see that the parameter e (called the *eccentricity*) may be represented just as

$$e = \left\{1 - \frac{E}{\min[U_{\text{ef}}(r)]}\right\}^{1/2}. \tag{3.62}$$

Analytical geometry tells us that Eq. (59), with $e < 1$, is one of the canonical representations of an *ellipse,* with one of its two focuses located at the origin. The fact that planets have such trajectories is known as the *1st Kepler's law*. Figure 7 shows the relations between the dimensions of the ellipse and the parameters p and e.[22]

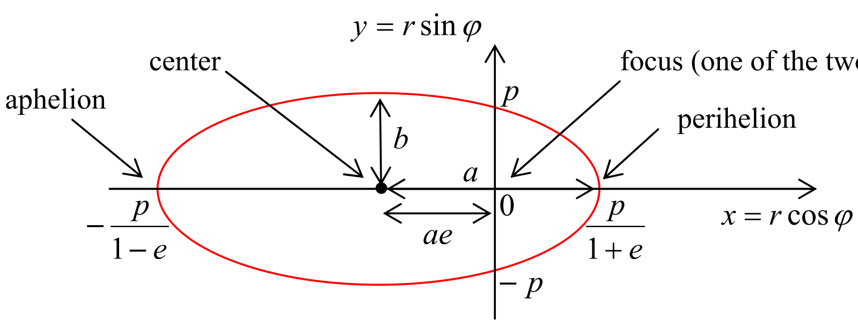

Fig. 3.7. Ellipse, and its special points and dimensions.

In particular, the *major semi-axis* a and the *minor semi-axis* b are simply related to p and e and hence, via Eqs. (60), to the motion integrals E and L_z:

$$a = \frac{p}{1-e^2} = \frac{\alpha}{2|E|}, \qquad b = \frac{p}{(1-e^2)^{1/2}} = \frac{L_z}{(2m|E|)^{1/2}}. \tag{3.63}$$

[20] Let me hope that the difference between the parameter p and the particle momentum's magnitude is absolutely clear from the context, so using the same (traditional) notation for both notions cannot lead to confusion.

[21] Mathematicians prefer a more solemn terminology: the parameter $2p$ is called the *latus rectum* of the ellipse.

[22] In this figure, the constant participating in Eqs. (58)-(59) is assumed to be zero. A different choice of the constant corresponds just to a different origin of φ, i.e. a constant turn of the ellipse about the origin.

As was mentioned above, at $E \to \min [U_{ef}(r)]$ the orbit is almost circular, with $r(\varphi) \cong r_0 \approx p$. On the contrary, as E is increased to approach zero (its maximum value for the closed orbit), then $e \to 1$, so that the aphelion point $r_{max} = p/(1 - e)$ tends to infinity, i.e. the orbit becomes extremely extended – see the magenta lines in Fig. 8.

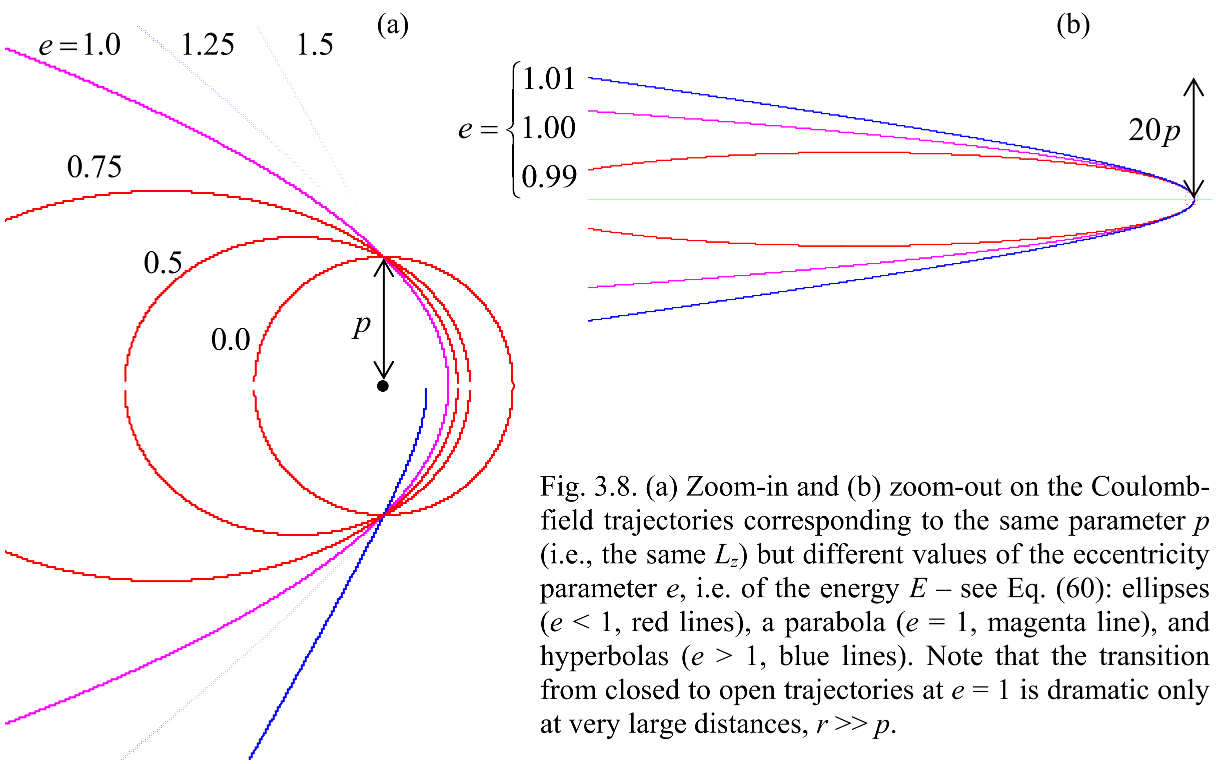

Fig. 3.8. (a) Zoom-in and (b) zoom-out on the Coulomb-field trajectories corresponding to the same parameter p (i.e., the same L_z) but different values of the eccentricity parameter e, i.e. of the energy E – see Eq. (60): ellipses ($e < 1$, red lines), a parabola ($e = 1$, magenta line), and hyperbolas ($e > 1$, blue lines). Note that the transition from closed to open trajectories at $e = 1$ is dramatic only at very large distances, $r >> p$.

The above relations enable, in particular, a ready calculation of the rotation period $\mathcal{T} \equiv \mathcal{T}_r = \mathcal{T}_\varphi$. (In the case of a closed trajectory, $\mathcal{T}_r$ and $\mathcal{T}_\varphi$ coincide.) Indeed, it is well known that the ellipse's area $A = \pi ab$. But according to the 2nd Kepler's law (40), $dA/dt = L_z/2m = \text{const}$. Hence

$$\mathcal{T} = \frac{A}{dA/dt} = \frac{\pi ab}{L_z/2m}. \tag{3.64a}$$

Using Eqs. (60) and (63), this important result may be represented in several other forms:

$$\mathcal{T} = \frac{\pi p^2}{(1-e^2)^{3/2}(L_z/2m)} = \pi\alpha\left(\frac{m}{2|E|^3}\right)^{1/2} = 2\pi a^{3/2}\left(\frac{m}{\alpha}\right)^{1/2}. \tag{3.64b}$$

Since for the Newtonian gravity (1.15), $\alpha = Gm_1m_2 = GmM$, at $m_1 << m_2$ (i.e. $m << M$), this constant is proportional to m, and the last form of Eq. (64b) yields the *3rd Kepler's law*: the periods of motion of different planets in the same central field, say that of our Sun, scale as $\mathcal{T} \propto a^{3/2}$. Note that in contrast to the 2nd Kepler's law (which is valid for any central field), the 1st and the 3rd Kepler's laws are potential-specific.

Now reviewing the above derivation of Eqs. (59)-(60), we see that they are also valid in the case of $E \geq 0$ – see the top horizontal line in Fig. 5 and its discussion above, if we limit the results to the physically meaningful range $r \geq 0$. This means that if the energy is exactly zero, Eq. (59) (with $e = 1$) is still valid for all values of φ (except for one special point $\varphi = \pi$ where r becomes infinite) and describes a *parabolic* (i.e. open) trajectory – see the magenta lines in Fig. 8.

Moreover, if $E > 0$, Eq. (59) is still valid within a certain sector of angles φ,

$$\Delta\varphi = 2\cos^{-1}\frac{1}{e} \equiv 2\cos^{-1}\left(1+\frac{2EL_z^2}{m\alpha^2}\right)^{-1/2} < \pi, \qquad \text{for } E > 0, \tag{3.65}$$

and describes an open, *hyperbolic* trajectory (see the blue lines in Fig. 8). As was mentioned earlier, such trajectories are typical, in particular, for particle scattering.

3.5. Elastic scattering

If $E > 0$, the motion is unbound for any realistic interaction potential. In this case, the two most important parameters of the particle trajectory are the *impact parameter* b and the *scattering angle* θ (Fig. 9), and the main task of the theory is to find the relation between them in the given potential $U(r)$.

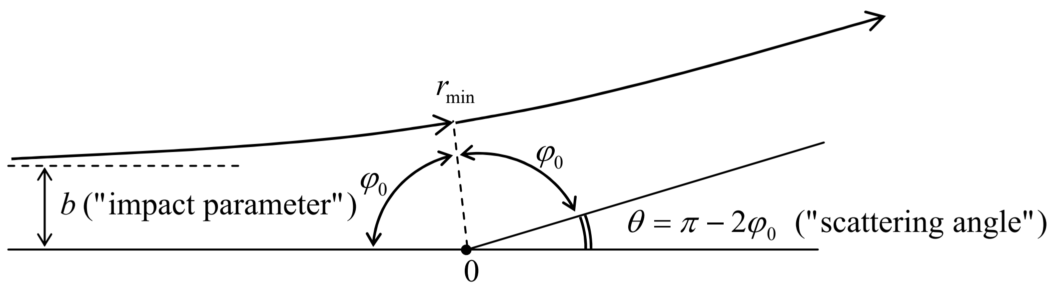

Fig. 3.9. Main geometric parameters of the scattering problem.

For that, it is convenient to note that b is related to the two conserved quantities, the particle's energy[23] E and its angular momentum L_z, in a simple way. Indeed, at $r >> b$, the definition $\mathbf{L} = \mathbf{r}\times(m\mathbf{v})$ yields $L_z = bmv_\infty$, where $v_\infty = (2E/m)^{1/2}$ is the initial (and hence the final) speed of the particle, so

$$L_z = b(2mE)^{1/2}. \tag{3.66}$$

Hence the angular contribution to the effective potential (44) may be represented as

$$\frac{L_z^2}{2mr^2} = E\frac{b^2}{r^2}. \tag{3.67}$$

Next, according to Eq. (48), the trajectory sections going from infinity to the nearest approach point ($r = r_{\min}$) and from that point to infinity, have to be similar, and hence correspond to equal angle changes φ_0 – see Fig. 9. Hence we may apply the general Eq. (48) to just one of the sections, say [$r_{\min}$, ∞], to find the scattering angle:

---

23 The energy conservation law is frequently emphasized by calling such process *elastic scattering*.

$$\theta = \pi - 2\varphi_0 = \pi - 2\frac{L_z}{(2m)^{1/2}}\int_{r_{\min}}^{\infty}\frac{dr}{r^2\left[E - U(r) - L_z^2/2mr^2\right]^{1/2}} \equiv \pi - 2\int_{r_{\min}}^{\infty}\frac{bdr}{r^2\left[1 - U(r)/E - b^2/r^2\right]^{1/2}}. \quad (3.68)$$

In particular, for the Coulomb potential (49), now with an arbitrary sign of α, we can use the same table integral as in the previous section to get[24]

$$|\theta| = \left|\pi - 2\cos^{-1}\frac{\alpha/2Eb}{\left[1+(\alpha/2Eb)^2\right]^{1/2}}\right|. \quad (3.69a)$$

This result may be more conveniently rewritten as

$$\tan\frac{|\theta|}{2} = \frac{|\alpha|}{2Eb}. \quad (3.69b)$$

Very clearly, the scattering angle's magnitude increases with the potential strength α, and decreases as either the particle energy or the impact parameter (or both) are increased.

The general result (68) and the Coulomb-specific relations (69) represent a formally complete solution of the scattering problem. However, in a typical experiment on elementary particle scattering, the impact parameter b of a single particle is unknown. In this case, our results may be used to obtain the statistics of the scattering angle θ, in particular, the so-called *differential cross-section*[25]

Differential cross-section

$$\boxed{\frac{d\sigma}{d\Omega} \equiv \frac{1}{n}\frac{dN}{d\Omega},} \quad (3.70)$$

where n is the average number of the *incident* particles per unit area, and dN is the average number of the particles *scattered* into a small solid angle interval $d\Omega$. For a uniform beam of initial particles, $d\sigma/d\Omega$ may be calculated by counting the average number of incident particles that have the impact parameters within a small range db:

$$dN = n\,2\pi b db. \quad (3.71)$$

Scattered by a spherically-symmetric center, which provides an axially-symmetric scattering pattern, these particles are scattered into the corresponding small solid angle interval $d\Omega = 2\pi|\sin\theta\, d\theta|$. Plugging these two equalities into Eq. (70), we get the following general geometric relation:

$$\frac{d\sigma}{d\Omega} = b\left|\frac{db}{\sin\theta d\theta}\right|. \quad (3.72)$$

In particular, for the Coulomb potential (49), a straightforward differentiation of Eq. (69) yields the so-called *Rutherford scattering formula* (reportedly, derived by R. H. Fowler):

Rutherford scattering formula

$$\boxed{\frac{d\sigma}{d\Omega} = \left(\frac{\alpha}{4E}\right)^2\frac{1}{\sin^4(\theta/2)}.} \quad (3.73)$$

[24] Alternatively, this result may be recovered directly from the first form of Eq. (65), with the eccentricity e expressed via the same dimensionless parameter $(2Eb/\alpha)$: $e = [1 + (2Eb/\alpha)^2]^{1/2} > 1$.

[25] This terminology stems from the fact that an integral (74) of $d\sigma/d\Omega$ over the full solid angle, called the *total cross-section* σ, has the dimension of the area: $\sigma = N/n$, where N is the total number of scattered particles.

This result, which shows very strong scattering to small angles (so strong that the integral that expresses the total cross-section

$$\boxed{\sigma \equiv \oint_{4\pi} \frac{d\sigma}{d\Omega} d\Omega} \qquad (3.74)$$

Total cross-section

is diverging at $\theta \to 0$)[26] and very weak *backscattering* (to angles $\theta \approx \pi$), was historically extremely significant: in the early 1910s, its good agreement with α-particle scattering experiments carried out by Ernest Rutherford's group gave a strong justification for his introduction of the *planetary model* of atoms, with electrons moving around very small nuclei – just as planets move around stars.

Note that elementary particle scattering is frequently accompanied by electromagnetic radiation and/or other processes leading to the loss of the initial mechanical energy of the system. Such *inelastic scattering* may give significantly different results. (In particular, the capture of an incoming particle becomes possible even for a Coulomb attracting center.) Also, quantum-mechanical effects may be important at the scattering of light particles with relatively low energies,[27] so the above results should be used with caution.

3.6. Exercise problems

3.1. For the system considered in Problem 2.6 (a bead sliding along a string with fixed tension $\mathscr{T}$, see the figure on the right), analyze small oscillations of the bead near the equilibrium.

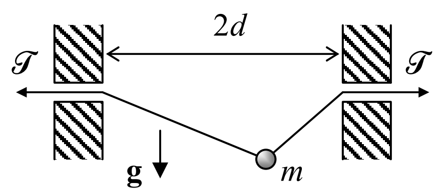

3.2. For the system considered in Problem 2.7 (a bead sliding along a string of a fixed length $2l$, see the figure on the right), analyze small oscillations near the equilibrium.

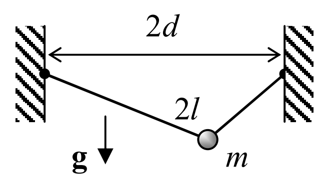

3.3. A bead is allowed to slide, without friction, along an inverted cycloid in a vertical plane – see the figure on the right. Calculate the frequency of its free oscillations as a function of their amplitude.

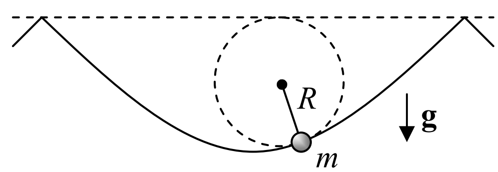

Hint: The simplest way to describe a cycloid is to express the Cartesian coordinates of its arbitrary point as functions of some parameter φ.[28] For the inverted cycloid shown in the figure on the right, such *parametric representation* is

$$x = R(\varphi + \sin\varphi), \qquad y = -R(1 + \cos\varphi).$$

[26] This divergence, which persists at the quantum-mechanical treatment of the problem (see, e.g., QM Chapter 3), is due to particles with very large values of b, and disappears at an account, for example, of any non-zero concentration of the scattering centers.

[27] Their discussion may be found in QM Secs. 3.3 and 3.8.

[28] This parameter may be understood as the angle of rotation of a circle of the radius R, rolled along a horizontal rail with $y = 0$ (see the dashed lines in the figure above), whose point moves along the cycloid..

3.4. Illustrate the changes of the fixed point set of our testbed system (Fig. 2.1), which was analyzed at the end of Sec. 3.2 of the lecture notes, on the so-called *phase plane* $[\theta, \dot{\theta}]$.

3.5. For a 1D particle of mass m, placed into the potential well $U(q) = \alpha q^{2n}$ (where $\alpha > 0$, and n is a positive integer), calculate the functional dependence of the particle's oscillation period $\mathcal{T}$ on its energy E. Explore the limit $n \to \infty$.

3.6. Two small masses m_1 and $m_2 \leq m_1$ may slide without friction over a horizontal surface. They are connected with a spring with an equilibrium length l and an elastic constant κ, and at $t < 0$ are at rest. At $t = 0$, the mass m1 gets a very short kick with impulse $\mathbf{P} \equiv \int \mathbf{F}(t)dt$ in a direction different from the spring's line. Calculate the largest and smallest magnitude of its velocity at $t > 0$.

3.7. Explain why the term $mr^2\dot{\varphi}^2/2$, recast in accordance with Eq. (42), cannot be merged with $U(r)$ in Eq. (38), to form an effective 1D potential energy $U(r) - L_z^2/2mr^2$, with the second term's sign opposite to that given by Eq. (44). We have done an apparently similar thing for our testbed bead-on-rotating-ring problem at the very end of Sec. 1 – see Eq. (6); why cannot the same trick work for the planetary problem? Besides a formal explanation, discuss the physics behind this difference.

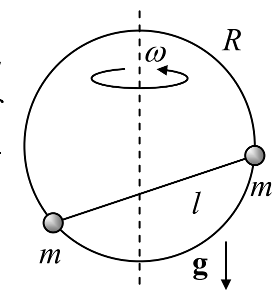

3.8. A system of two equal masses m on a light rod of a fixed length l (frequently called a *dumbbell*) can slide without friction along a vertical ring of radius R, rotated about its vertical diameter with a constant angular velocity ω – see the figure on the right. Derive the condition of stability of the lower horizontal position of the dumbbell.

3.9. Analyze the dynamics of the so-called *spherical pendulum* – a point mass hung, in a uniform gravity field $\mathbf{g}$, on a light cord of length l, with no motion's confinement to a vertical plane. In particular:

(i) find the integrals of motion and reduce the problem to a 1D one,
(ii) calculate the time period of the possible circular motion around the vertical axis, and
(iii) explore small deviations from the circular motion. (Are the pendulum's orbits closed?)[29]

3.10. If our planet Earth was suddenly stopped in its orbit around the Sun, how long would it take it to fall on our star? Solve this problem using two different approaches, neglecting the Earth's orbit eccentricity and the Sun's size.

3.11. The orbits of Mars and Earth around the Sun may be well approximated as coplanar circles,[30] with a radii ratio of 3/2. Use this fact, and the Earth's year duration, to calculate the time of travel to Mars when spending the least energy on the spacecraft's launch. Neglect the planets' size and the effects of their own gravitational fields.

---

[29] Solving this problem is very good preparation for the analysis of the symmetric top's rotation in Sec. 4.5.
[30] Indeed, their eccentricities are close to, respectively, 0.093 and 0.0167.

3.12. Derive first-order and second-order differential equations for the reciprocal distance $u \equiv 1/r$ as a function of φ, describing the trajectory of a particle's motion in a central potential $U(r)$. Spell out the latter equation for the particular case of the Coulomb potential (49) and discuss the result.

3.13. For the motion of a particle in the Coulomb attractive field ($U(r) = -\alpha/r$, with $\alpha > 0$), calculate and sketch the so-called *hodograph*[31] – the trajectory followed by the head of the velocity vector $\mathbf{v}$, provided that its tail is kept at the origin.

3.14. Prove that for an arbitrary motion of a particle of mass m in the Coulomb field $U = -\alpha/r$, the vector $\mathbf{A} \equiv \mathbf{p}\times\mathbf{L} - m\alpha\mathbf{n}_r$ (where $\mathbf{n}_r \equiv \mathbf{r}/r$) is conserved.[32] After that:

(i) spell out the scalar product $\mathbf{r}\cdot\mathbf{A}$ and use the result for an alternative derivation of Eq. (59), and for a geometric interpretation of the vector $\mathbf{A}$;

(ii) spell out $(\mathbf{A} - \mathbf{p}\times\mathbf{L})^2$ and use the result for an alternative derivation of the hodograph diagram discussed in the previous problem.

3.15. For a particle moving in the following central potential:

$$U(r) = -\frac{\alpha}{r} + \frac{\beta}{r^2},$$

(i) for positive α and β, and all possible ranges of energy E, calculate the orbit $r(\varphi)$;

(ii) prove that in the limit $\beta \to 0$, for energy $E < 0$, the orbit may be represented as a slowly rotating ellipse;

(iii) express the angular velocity of this slow rotation via the parameters α and β, the particle's mass m, its energy E, and the angular momentum L_z.

3.16. A star system contains a much lighter planet and an even much smaller mass of dust. Assuming that the attractive gravitational potential of the dust is spherically symmetric and proportional to the square of the distance from the star,[33] calculate the slow precession it gives to a circular orbit of the planet.

3.17. A particle is moving in the field of an attractive central force with the potential

$$U(r) = -\frac{\alpha}{r^n}, \qquad \text{where } \alpha n > 0.$$

For what values of n, the circular orbits are stable?

3.18. Determine the condition for a particle of mass m, moving under the effect of a central attractive force

---

[31] The use of this notion for the characterization of motion may be traced back at least to an 1846 treatise by W. Hamilton. Nowadays, it is most often used in applied fluid mechanics, in particular meteorology.

[32] This fact, first proved in 1710 by Jacob Hermann, was repeatedly rediscovered during the next two centuries. As a result, the most common name of **A** is, rather unfairly, the *Runge-Lenz vector*.

[33] As may be readily shown from the gravitation version of the Gauss law (see, e.g., the model solution of Problem 1.7), this approximation is exact if the dust density is constant between the star and the planet.

$$\mathbf{F} = -\alpha \frac{\mathbf{r}}{r^3} \exp\left\{-\frac{r}{R}\right\},$$

where α and R are positive constants, to have a stable circular orbit.

3.19. A particle of mass m, with an angular momentum L_z, moves in the field of an attractive central force with a distance-independent magnitude F. If the particle's energy E is slightly higher than the value $E_{\min}$ corresponding to its circular orbit, what is the time period of its radial oscillations? Compare the period with that of the circular orbit at $E = E_{\min}$.

3.20. A particle may move without friction, in the uniform gravity field $\mathbf{g} = -g\mathbf{n}_z$, over an axially-symmetric surface that is described, in the cylindrical coordinates $\{\rho, \varphi, z\}$, by a smooth function $Z(\rho)$ – see the figure on the right. Derive the condition of stability of circular orbits of the particle around the symmetry axis z, with respect to small perturbations. For the cases when the condition is fulfilled, find out whether the weakly perturbed orbits are open or closed. Spell out your results for the following particular cases:

(i) a conical surface with $Z = \alpha\rho$,
(ii) a paraboloid with $Z = \kappa\rho^2/2$, and
(iii) a spherical surface with $Z^2 + \rho^2 = R^2$, for $\rho < R$.

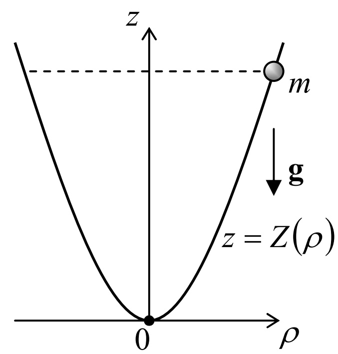

3.21. The gravitational potential (i.e. the gravitational energy of a unit probe mass) of our Milky Way galaxy, averaged over interstellar distances, is reasonably well approximated by the following axially symmetric function:

$$\phi(r,z) = \frac{V^2}{2} \ln\left(r^2 + \alpha z^2\right),$$

where r is the distance from the galaxy's symmetry axis and z is the distance from its central plane, while V and $\alpha > 0$ are constants.[34] Prove that circular orbits of stars in this gravity field are stable, and calculate the frequencies of their small oscillations near such orbits, in the r- and z-directions.

3.22. For particle scattering by a repulsive Coulomb field, calculate the minimum approach distance $r_{\min}$ and the velocity $v_{\min}$ at that point, and analyze their dependence on the impact parameter b (see Fig. 9) and on the initial velocity v_∞ of the particle.

3.23. A particle is launched from afar, with an impact parameter b, toward an attracting center creating the potential

$$U(r) = -\frac{\alpha}{r^n}, \quad \text{with } n > 2 \text{ and } \alpha > 0.$$

(i) For the case when the initial kinetic energy E of the particle is barely sufficient for escaping its capture by this attracting center, express the minimum approach distance via b and n.

(ii) Calculate the capture's total cross-section and explore its limit at $n \to 2$.

[34] Just for the reader's reference, these constants are close to, respectively, 2.2×10^5 m/s and 6.

3.24. A small body with an initial velocity v_∞ approaches an atmosphere-free planet of mass M and radius R.

(i) Find the condition on the impact parameter b for the body to hit the planet's surface.

(ii) If the body barely avoids the collision, what is its scattering angle?

3.25. Calculate the differential and total cross-sections of the classical elastic scattering of small particles by a hard sphere of radius R.

3.26. The most famous[35] confirmation of Einstein's general relativity theory has come from the observation, by A. Eddington and his associates, of star light's deflection by the Sun, during the May 1919 solar eclipse. Considering light photons as classical particles propagating with the speed of light, $v_0 \rightarrow c \approx 3.00\times10^8$m/s, and using the astronomic data for the Sun's mass ($M_S \approx 1.99\times10^{30}$kg) and radius ($R_S \approx 6.96\times10^8$m), calculate the non-relativistic mechanics' prediction for the angular deflection of the light rays grazing the Sun's surface.

3.27. Generalize the expression for the small angle of scattering, obtained in the solution of the previous problem, to a spherically symmetric but otherwise arbitrary potential $U(r)$. Use the result to calculate the differential cross-section of small-angle scattering by the potential $U = C/r^n$, with integer $n > 0$.

Hint: You may like to use the following table integral: $\int_1^\infty \frac{d\xi}{\xi^{n+1}\left(\xi^2 - 1\right)^{1/2}} = \pi^{1/2}\frac{\Gamma(n/2+1/2)}{n\Gamma(n/2)}$.

[35] It was not the first confirmation, though. The first one came four years earlier from Albert Einstein himself, who showed that his theory may qualitatively explain the difference between the rate of Mercury orbit's precession, known from earlier observations, and the non-relativistic theory of that effect.